Predicting the Weather by Watching Aeroplanes: Applying Refractive Techniques to Air-plane ADSB Radio Wave Signals in the Lower Troposphere for Determining Relative Humidities.

Matthew Evans

27th March 2019

Abstract

Various wave properties were investigated by exploring water waves in a ripple tank and studying the diffraction of laser light. A value of 0.18 ± 0.05 ms^{-1} for water wave speed at varying frequencies and a fixed depth of $h = 1.0 \pm 0.3$ cm was obtained and the one generated by using $v \approx \sqrt{gh}$ [4] was 0.3 ± 0.1 ms^{-1}. The angles of incidence and reflection for the reflection of water waves at a barrier were found to be $41 \pm 2^{\circ}$ and $41 \pm 2^{\circ}$ respectively. The water wave speed was also investigated at a fixed frequency of 20 Hz with varying depths allowing a value of 4.4 ± 0.1 ms^{-2} for the acceleration due to gravity to be determined with the known value as 9.8 ms^{-2}. The value for the wave speed at varying frequencies was different to the one expected lying outside the uncertainty range, also the value of g was different to the known value however, the angle of incidence and reflection were shown to be equal to each other. Experimental values determined for the wavelength of the laser light source for the single and double-slit configurations was found to be 652.1 ± 0.7 nm and 655.71 ± 0.03 nm respectively, using a 0.3mm aperture, a slit width of $a = 0.04$ mm and slit separation of $d = 0.5$ mm: the value of the device is 650 ± 10 nm [8]. These values compare well with the device value along with other single and double-slit configurations generating wavelengths that compared well with the device value but, all the uncertainties of the experimental values of the wavelength were underestimated. By understanding water waves and electromagnetic waves, hydroelectric power and chemical spectra analysis could be optimised for the benefit of many modern day appliances.

Contents

1 Introduction

The Earth's weather in the troposphere is a complicated dynamical system with many factors playing a crucial role in its development. Four of the most important are temperature, pressure, wind velocity and humidity. During this project, the relative humidity (RH) of the troposphere was investigated by treating it as constant (homogeneous) in order to obtain a relative humidity values. By obtaining values for the relative humidity many benefits can be obtained. One benefit might be that by knowing the relative humidity this could be used in our day-to-day lives to gain an idea of what the weather will be on a particular day, another is that this could give more accurate rainfall patterns allowing farmers to optimise weather conditions when planting crops. Furthermore, the prediction of heavy rainfall could be predicated — saving lives in the case of serious flooding. Thus, the relative humidity of the troposphere is of crucial interest to weather forecasters and this project was carried out in association with the Met Office to help develop their forecasting techniques.

At present, this is difficult to measure directly and only a small number of aircraft have such devices, for example Aircraft Meteorological Data Relay (AMDAR), on board [1] and these are often expensive which limits further opportunities using this method of measurement. An alternative approach in measuring humidity which has been proposed [1] is to use Automatic Dependent Surveillance Broadcast (ADSB) signals from air planes where many of these aircraft have this equipment on board. Therefore, these broadcasts containing aircraft information such as position, velocity, altitude and so on, can be continually obtained by ground monitoring facilities from many different aircraft. By studying how ADSB radio wave signals are refracted within the Earth's lower atmosphere, this could provide a way of obtaining the water vapour distribution thus give relative humidity values.

2 Theory

3 Method

3.1 Mechanical Waves

3.2 Electromagnetic Waves

4 Results

Figure 1 shows two plots of radial distance from the centre of the Earth, R against the increment angle measured from the vertical through the centre of the Earth, θ for a given observed angle range of 0.1° - 0.11° for early (Figure 1a) and late (Figure 1b) times of observation on 26$^{\text{nd}}$ August 2019 starting at 11:45 am. Furthermore, Figure 2 and Figure 3 show additional plots of these R and θ positions for different observed angle ranges of 0.3° - 0.31° and 0.5° - 0.51° respectively. Again, the early times of observation are shown for these different observed angles ranges in Figure 2a and Figure 3a at observed angle ranges of 0.3° - 0.31° and 0.5° - 0.51° respectively. Whereas the late times are shown in Figure 2b and Figure 3b for the observed angle ranges of 0.3° - 0.31° and 0.5° - 0.51° respectively. All these plot values are shown for the plane positions, in addition to the model relative humidity curves for 0%, 100% and the best fitting relative humidity curve for the plane positions.

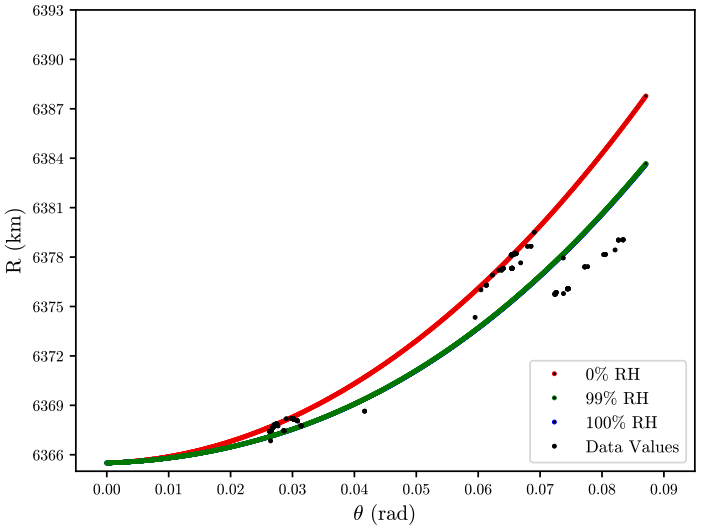

(a) R vs θ for early times (the first 5000s) of observation.

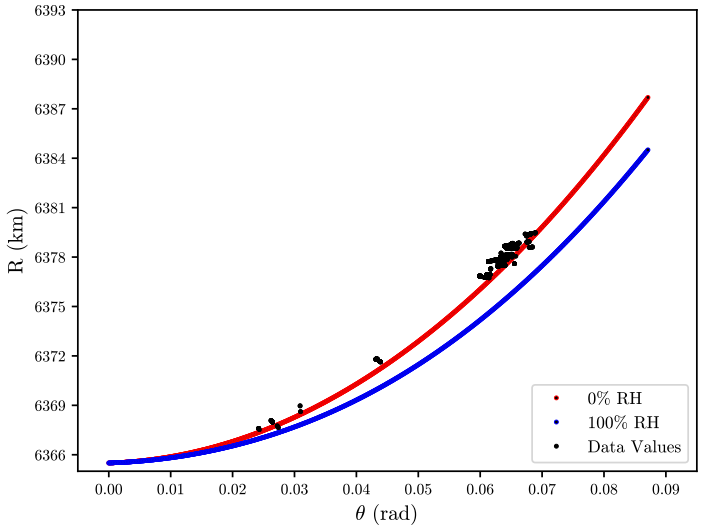

(b) R vs θ for late times (the last 5000s) of observation.

Figure 1: Plots of radial distance, R against increment angle, θ from the vertical through the centre of the Earth for plane positions (shown in black) at a given observed angle range between 0.1° - 0.11° for early and late times of observation.

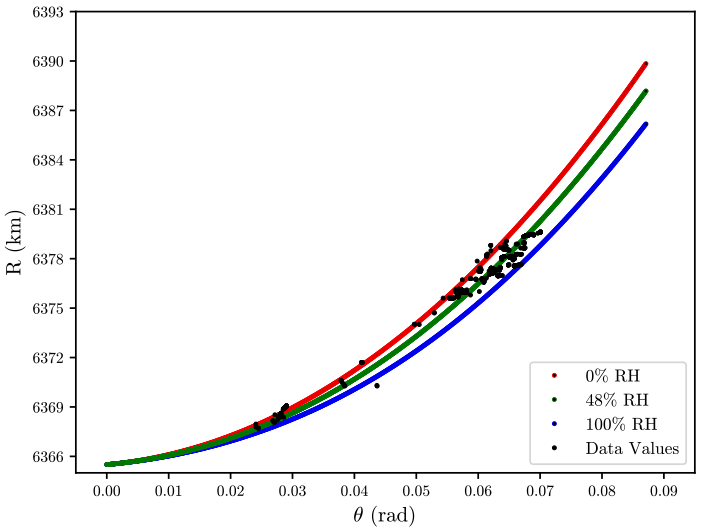

(a) R vs θ for early times (the first 5000s) of observation.

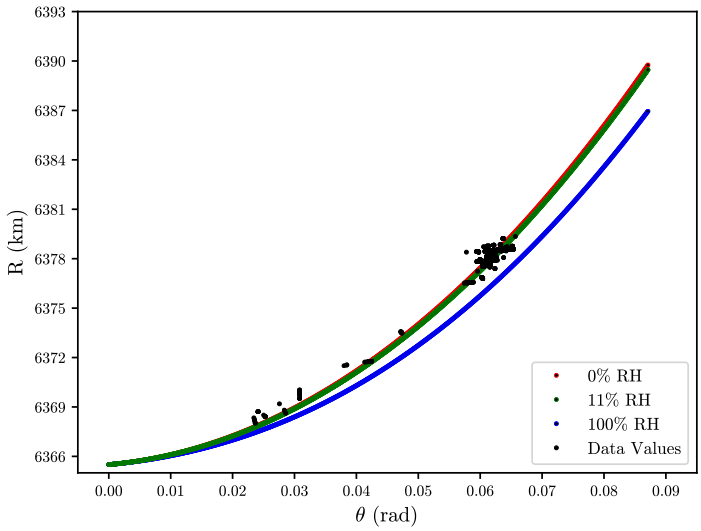

(b) R vs θ for late times (the last 5000s) of observation.

Figure 2: Plots of radial distance, R against increment angle, θ from the vertical through the centre of the Earth for plane positions (shown in black) at a given observed angle range between 0.3° - 0.31° for early and late times of observation.

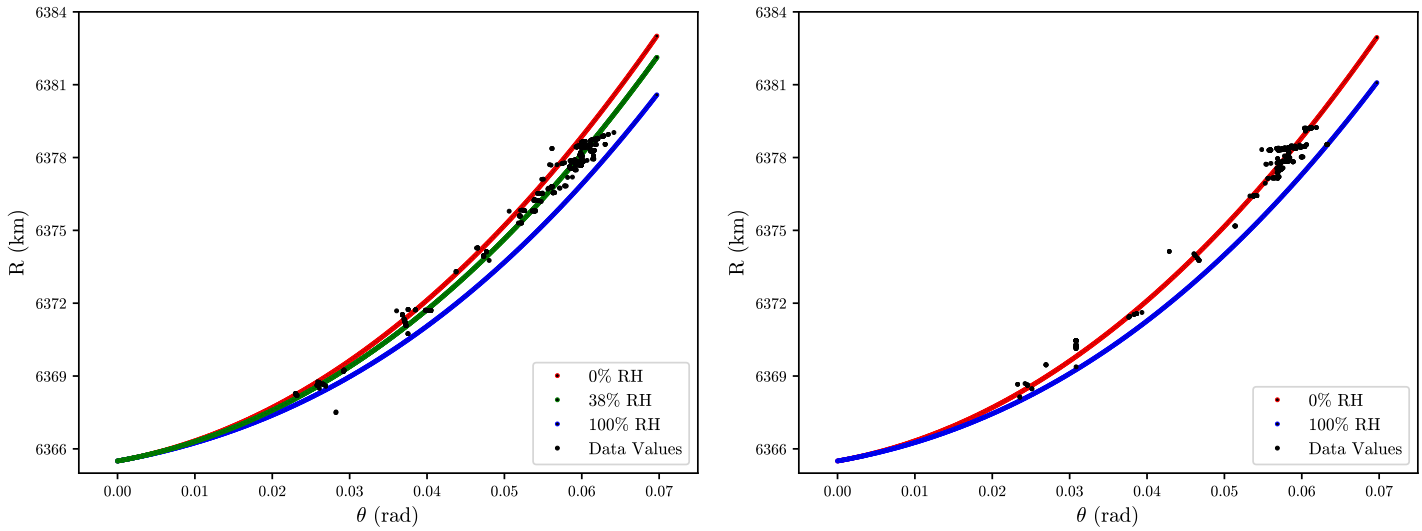

(a) R vs θ for early times (the first 5000s) of observation.

(b) R vs θ for late times (the last 5000s) of observation.

Figure 3: Plots of radial distance, R against increment angle, θ from the vertical through the centre of the Earth for plane positions (shown in black) at a given observed angle range between 0.5° - 0.51° for early and late times of observation.

Table 1 compares the obtained values for the relative humidity from the best fitting (green) curves in Figure 1a, Figure 2a and Figure 3a to the mean of the actual relative humidities obtained from [7] along with their estimated errors for each of the observed angle ranges at early times of observation.

Table 1: A table comparing generated relative humidities (RH) from an interpolative and least squares method for the various different observed angle, ϕ_0 ranges investigated to the mean of the actual RH values given by [7] for the early times of observation (first 5000s).

Observed Angle Range ϕ_0 (°)	Generated RH (%)	Actual RH (%) [7]
0.10 - 0.11	99 ± 8	74 ± 4
0.30 - 0.31	48 ± 3	74 ± 4
0.50 - 0.51	38 ± 3	74 ± 4

Table 2 compares the obtained values for the relative humidity from the best fitting (green) curves in Figure 1b, Figure 2b and Figure 3b to the mean of the actual relative humidities obtained from [7] along with their estimated errors for each of the observed angle ranges at late times of observation.

Table 2: A table comparing generated relative humidities (RH) from an interpolative and least squares method for the various different observed angle, ϕ_0 ranges investigated to the mean of the actual RH values given by [7] for the late times of observation (last 5000s).

Observed Angle Range ϕ_0 (°)	Generated RH (%)	Actual RH (%) [7]
0.10 - 0.11	-	77 ± 5
0.30 - 0.31	$11 \pm <1$	77 ± 5
0.50 - 0.51	-	77 ± 5

The errors for the actual relative humidities for the early and late times of observation, given by [7], were estimated by using the error on the mean value of the relative humidity using,

$$\delta RH = \frac{\sigma(RH)}{\sqrt{N_{RH}}} \tag{1}$$

where $\sigma(RH)$ is the standard deviation of the average actual relative humidity ($\overline{RH}$) and N_{RH} is the number of RH values used to determine these averages.

However, the errors for the generated relative humidities were estimated in Table 1 and Table 2 by using the error on the mean for the baseline temperature T_b [7], baseline pressure P_b [7] and observed angle ϕ_0. The following were used to obtain these errors

$$\delta T_b = \frac{\sigma(T_b)}{\sqrt{N_{T_b}}} \tag{2}$$

$$\delta P_b = \frac{\sigma(P_b)}{\sqrt{N_{P_b}}} \tag{3}$$

$$\delta \phi_0 = \frac{0.03}{\sqrt{N_{\phi_0}}} \tag{4}$$

where $\sigma(T_b)$, $\sigma(P_B)$ are the standard deviations of the baseline temperature and pressure respectively, 0.03 is the known error in the observed angle as given by internal project communications, N_{T_b}, N_{P_b} and N_{ϕ_0} are the number of baseline temperature, pressure and observed angle readings considered.

These estimated errors given in (2), (3) and (4) were added to the mean values for the baseline temperature, baseline pressure and observed angle when calculating the refracted ray path using the appropriate computer program. This gave an upper bound on the relative humidity value. Thus, the difference between the upper bound of the relative humidity and the relative humidity generated by using the average of these values gave an estimated error for the generated relative humidity value.

5 Discussion

The results for the determined relative humidities given for the early and late part of the observations in Table 1 and Table 2 respectively show that the relative humidity does vary as a function of time. This is due to the fact that later in the day, the temperature and pressure decreases causing a change in the relative humidity as anticipated in Section 2.

By considering the early part of the day, the relative humidities given in Table 1 show discrepencies when compared with the actual relative humidities. The corresponding graphs displaying these best fitting relative humidity curves in Figure 1a, Figure 2a and Figure 3a visually show these discrepencies. For example, in Figure 2a and Figure 3a show that indeed the plane positions are grouped towards a lower relative humidity. However, when compared to the actual values displayed in Table 1 these generated values are much lower. This could be due to the fact that the relative humidity cannot be treated as a constant, homogenous value. Instead, the relative humidity could be varying as a function of many different factors; such as tempearture, pressure, height, etc.

Furthermore, by considering Figure 1a the plane positions seem to be forming two distinct relative humidity curves. This shows that the relative humidity does indeed seem to be different for a specific observed angle range. In this case, there is a shallow observed angle range 0.1° - 0.11° above the horizon. From the discussion presented in Section 2 this is where most of the refraction occurs due to the denser atmosphere nearer the Earth's surface. Therefore, it would be expected that more refraction would occur because the ADSB signal spends more time in the lower part of the atmosphere for these small observed angles above the horizon according to Section 2 FIGURE EARTH. This is shown by the bottom set of plane position data values in Figure 1a. However, there is also a set of points that indicate a higher relative humidity. This was investigated further and additional measurements, using the latitude and longitude plane positions, show that the relative humidty, as well as depending on time, also depends on upon the horizontal direction (azimuthal angle). Figure 4 shows a plot of latitude against longitude for the observed angle range 0.1° - 0.11° for early observation times.

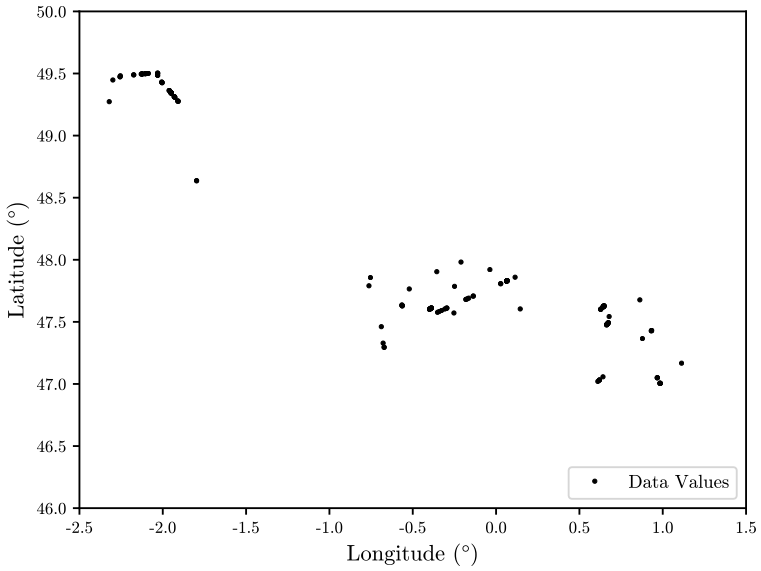

Figure 4: A plot showing the latitude and longitude plane positions during the early part of observations (first 5000s) for the observed angle range 0.1° - 0.11°.

Figure 4 shows that for this given observed angle range there are three distinct horizontal regions for these plane positions. This shows that the relative humidity also depends upon the horizontal orientation as well as time.

Analysing the results for the determined relative humidities given for the late part of the observations in Table 2 show further discrepencies when compared to the actual relative humidites. Many of these relative humidities could not be determined due to the nature of the graphs displayed in Figure 1b, and Figure 3b. These plots show that the plane positions would yield a best fit relative humidity curve that would be less than 0%. This further indicates that the relative humidity cannot be treated as an absolute constant value and that the gradient of the relative humidity curves in addition to how they curves vary with height should be considered.

By considering the refractivity as a function of height, this would mean that a higher ground level relative humidity would give a steeper fall-off gradient with height due to the refractivity relations given in Section 2. For the plots Figure 1b, Figure 2b and Figure 3b we see that the generated relative humidities are less than 0%. Therefore, a systematic shift would be required for the plane positions, so that a model refractivity curve with a low value of relative humidity could be used to represent the data. This would display the same shallow gradient characterisitcs of the plane position data for low relative humidities, but translated to a higher refractivity/relative humidity.

This change in relative humidity with height above ground level for the translated curve, this would result in an intially rising relative humidity with height. However, this would have to fall off after some height as this translated refractivity curve would interesect the 100% refractivity curve (which has a steeper fall off gradient with height) because this translated curve would not be able to go above 100% due to the definition of relative humidity given in Section 2. Therefore, this means that the relative humidity would initially rise and then fall off again when this intersection between the two refractivity curves against height occurs. Furthermore, this analysis of the results given in Table 2 shows further evidence that the relative humidity cannot be treated as a constant, homogenous value.

6 Conclusion

References

[1] Stone E.K and Kitchen M, 2015, Introducing an Approach for Extracting Temperature from Aircraft GNSS, Journal of Atmospherics and Oceanic Technology, Vol 32, pages 736 - 743. and Pressure Altitude Reports in ADS-B Messages

[2] College of Engineering, Mathematics and Physical Sciences, University of Exeter, PHY2026, *Diffraction and Interference Worksheet* (Accessed 8th February 2019).

[3] Young, Hugh D and Freedman, Roger A, *University Physics*, 13th Edition, 2014, Chapter 36, pages 1312 - 1322.

[4] Barber N.F, *Water Waves*, 1st Edition, 1969, Chapter 3, pages 36 - 55.

[5] Pedrotti F.L, Pedrotti S.J, *Introduction to Optics*, (Pearson International Edition) 3rd Edition, 2006, Chapter 11-1: *Diffraction from a Single Slit*, pages 268 - 273.

[6] Pedrotti F.L, Pedrotti S.J, *Introduction to Optics*, (Pears onInternational Edition) 3rd Edition, 2006, Chapter 11-5: *Double-Slit Diffraction*, pages 281 - 284.

[7] Met Office Weather Observations Website, 22nd November 2019, `https://wow.metoffice.gov.uk/`.)

[8] *Red Diode Laser - Basic Optics - OS-8525A*, `https://www.pasco.com/prodCatalog/OS/OS-8525_red-diode-laser-basic-optics/index.cfm?fbclid=IwAR3gzuNSAoumEZpwYZQO6tX3j1nLhTtLYklX5U6V6HHw5xyHKdszO1ID00I` (Accessed 15th March 2019).